processes

MDPI

Article

Research on the Main Causes of Water Channeling in High-Pressure Water Injection of Low-Permeability Reservoirs and the Regulation Strategies of the Seepage Field

Kai Yang [1,2,3,4], Hualei Xu [1,2,4,*], Jianyu Li [1,2,4], Ziqi Chen [1,2,4], Jie Wang [1,2,4] and Houshun Jiang [1,2,4]

1 Cooperative Innovation Center of Unconventional Oil and Gas, Yangtze University, Wuhan 430100, China
2 Hubei Key Laboratory of Oil and Gas Drilling and Production Engineering, Yangtze University, Wuhan 430100, China
3 State Key Laboratory of Petroleum Resources and Engineering, China University of Petroleum (Beijing), Beijing 102249, China
4 State Key Laboratory of Low Carbon Catalysis and Carbon Dioxide Utilization, Yangtze University, Wuhan 430100, China
* Correspondence: hualeixu@yangtzeu.edu.cn

Abstract

High-pressure water injection (HPWI) can rapidly replenish the formation energy of low-permeability reservoirs, but it may trigger multi-scale fractures, leading to premature water breakthrough between injection and production wells. To identify the main causes and regulate the mainstream line (i.e., the preferential flow path with the highest streamline density/flow rate), a two-zone and five-point numerical model was developed. This model couples the static damage zone (dominated by micro-fractures) and the fracture development zone (dominated by macro-fractures). Through sensitivity analysis, the ways in which micro-fracture damage and macro-fracture geometry control the evolution of seepage patterns and the risk of water breakthrough were quantified. The results show that in the representative scenarios of this paper, micro-fracture damage is mainly associated with an increased risk of water breakthrough by forming equivalent weakening zones and enhancing the directional extension trend of main fractures. The scale of macro-fractures has the strongest correlation with the water breakthrough response. When the fracture scale increases to a certain proportion close to the well spacing, the seepage mode changes from "fracture + matrix cooperation" to "main-fracture-dominated short-circuit channel". Based on this, a design and verification of a combined control scheme of "chemical profile control + cyclic water injection" was proposed and carried out in well groups with high water cut and strong channeling. Simulations show that this combination helps to weaken the flow conductivity of preferential channels and improve the uniformity of the flow field. This paper can provide technical support for the prevention, control, and early warning of water breakthrough and the regulation of main flow lines in the high-pressure water injection development of similar low-permeability reservoirs.

Keywords: low-permeability reservoirs; high-pressure water injection; main flow lines; seepage flow patterns; numerical simulation

Check for updates

Academic Editor: Liyun Yang

Received: 27 January 2026
Revised: 25 February 2026
Accepted: 6 March 2026
Published: 11 March 2026

Correction Statement: This article has been republished with a minor change. The change does not affect the scientific content of the article and further details are available within the backmatter of the website version of this article.

Copyright: © 2026 by the authors. Licensee MDPI, Basel, Switzerland. This article is an open access article distributed under the terms and conditions of the Creative Commons Attribution (CC BY) license.

1. Introduction

Low-permeability reservoirs have abundant resource reserves, and their efficient development is of great strategic significance for safeguarding national energy security [1–3]. However, such reservoirs generally have prominent problems such as insufficient natural

energy, high startup pressure, and rapid production decline. It is difficult to achieve long-term stable and efficient development through conventional development methods [4–6]. High-pressure water injection (HPWI), as an important technology for improving the development efficiency of low-permeability reservoirs, can quickly replenish energy and enhance oil recovery within a relatively short period by injecting water at a high flow rate and high speed at a pressure higher than or close to the formation fracture pressure [7,8]. However, at the same time, the thermo-mechanical coupling effect and rapid pore pressure fluctuations caused by high-pressure water injection can easily lead to the damaging of the reservoir rock structure and induce the development of multi-scale fracture networks, which in turn form preferential inter-well water channeling paths [9]. Once such channels are formed, they will not only significantly reduce the water-flooding sweep volume, but also easily cause sudden water channeling and flooding in production wells, resulting in intensified ineffective water circulation and a sharp decline in development efficiency. This has become one of the key technical bottlenecks restricting the efficient development of low-permeability reservoirs [10–12].

Existing studies generally suggest that the formation of water channeling under HPWI conditions is jointly controlled by geological and engineering factors. The main controlling factors are mainly reflected in aspects such as reservoir properties, fluid characteristics, and development methods [13–15]. From the engineering perspective, large-pressure-difference, short-term and continuous large-scale injection will significantly increase the near-well pressure drop and seepage shear effect. This may cause the matrix near the injection well to fracture or induce the development of micro-fractures, increase the pore-throat scale and equivalent permeability, and thus change the injection capacity and the structure of the seepage channel. Zhu et al. [16] established an oil–water two-phase flow model considering the threshold pressure gradient to evaluate the high-pressure water injection capacity. They pointed out that the injection performance is not only controlled by the physical properties of the matrix, but also closely related to the structural characteristics of the stimulated zone. Li et al. [17] systematically clarified the causes of the differences in high-pressure water injection effects from two aspects: geological factors (heterogeneity, development of dominant channels) and engineering factors (injection rate, induced micro-fractures). From a geological perspective, the spatial distribution and geometric irregularities of reservoir heterogeneity and natural fractures can significantly control the dominant seepage direction and the shape of the water-flooding front. This makes the displacement process exhibit non-uniform advancement and easily form equivalent high-permeability strips locally, which in turn induces inter-well channeling. In response to this problem, Mao et al. [18] started from the perspective of microscopic seepage and quantitatively evaluated the controlling effect of reservoir heterogeneity on the uniformity of water-flooding front advancement, early water breakthrough, and the spatial distribution of remaining oil. Further research shows that, when other conditions remain unchanged, as the permeability contrast of the reservoir increases, the remaining oil saturation increases significantly, and the sweep area of HPWI shows the characteristics of “becoming narrower and extending longer”. This indicates that in areas with strong planar heterogeneity, the injected water is more likely to migrate along a single high-permeability strip, thus weakening the overall oil-displacement effect [19,20]. Overall, geological heterogeneity and natural fractures provide the “basis for directionality and connectivity”, while engineering injection loads provide the “energy input and trigger for structural transformation”. The combination of the two drives the redistribution of the pressure field and saturation field, ultimately leading to the formation of preferential seepage zones and potentially causing inter-well channeling. However, in the multi-scale collaborative evolution process of micro-fracture damage and macroscopic fracture connection under HPWI conditions, there is still a lack of systematic

and quantifiable understanding of the threshold conditions for the formation of water channeling paths and their mechanism of action on the evolution of the main streamline.

As the development progresses, the preferential channels often exhibit self-strengthening characteristics under continuous injection–production actions, gradually forming a short-path seepage pattern that is difficult to redirect. This reduces the marginal effect of conventional profile control and flooding or single water injection system adjustment [21]. Against this background, the research focus of "main streamline" regulation has shifted from local and passive plugging to the active reconstruction of the flow field. Its core lies in identifying and weakening the preferential seepage paths that contribute the main flow. Through the collaborative optimization of the well pattern and the injection–production system, a pressure-seepage field structure that is more conducive to multi-directional flow diversion and uniform sweep is reconstructed [22,23]. Related research mainly unfolds along two technical routes: First there is the overall optimization centered on the well pattern and injection–production parameters. Zhang et al. [24] systematically regulated the flow field with strong seepage differences from aspects such as well pattern optimization, adjustment of injection–production parameters, and cyclic water injection, achieving good results in water control and oil stabilization. Second, there is the identification and regulation of the main streamline using streamline characterization and visualization as tools. Yin et al. [25] used streamline simulation and three-dimensional flow field visualization to reveal the differences in water-flooding efficiency under irregular well patterns and improved the sweep efficiency by optimizing the water injection parameters. BuKhamseen et al. [26] combined the streamline method with fuzzy logic to construct a water injection optimization decision-making model, which provided a new implementation path for the collaborative regulation of main and non-main streamlines under complex flow field conditions. Nevertheless, affected by factors such as strong heterogeneity of low-permeability reservoirs, large differences among well groups, and multi-scale coupling of fractures and matrix, the existing channeling control technologies still have deficiencies in terms of engineering pertinence and effect persistence. They often exhibit fluctuating regulation effects, with limited stability and replicability.

In summary, existing research has made progress in understanding the relationship between HPWI-induced fractures and water channeling. However, there is still a lack of a quantitative framework that integrates micro-fracture damage, macroscopic fracture connectivity, and the evolution of dominant channels in the seepage field. Therefore, it is difficult to provide threshold criteria for early warning and control design. To address this, this paper proposes and tests the following hypotheses: H1: Micro-fracture damage mainly reduces the threshold for macroscopic fracture connectivity by forming directional equivalent weakening zones. H2: When the half-length of macroscopic fractures reaches a certain proportion of the well spacing, the seepage pattern undergoes a transition, leading to rapid water channeling. H3: Through "profile control + cyclic water injection", the dominance of the main streamline can be weakened, and multi-directional flow diversion can be reestablished, thereby improving the sweep efficiency. Based on this, this paper (1) constructs a coupled model of a dual-region five-spot well pattern to depict the linkage between the damaged zone and the fracture-developed zone; (2) presents the criteria for the critical scale of macro-fractures and water breakthrough risk; and (3) proposes and verifies a combined strategy for mainstream line regulation, providing operational guidance for water breakthrough control under the condition of HPWI in low-permeability reservoirs.

2. Mechanism and Model

2.1. Introduction to the Research on the Distribution of Block Fractures

During the high-pressure water injection development of the ultra-low permeability reservoir in Block A of Oilfield S, the energy concentration effect in the high-pressure area is significant, which easily induces the formation of new fractures or promotes the reconnection of the original natural fracture network, resulting in an obvious high-conductivity channel for fluid channeling between the injection well and the production well [27]. Before HPWI, the ultra-low permeability reservoir in Block A is mainly composed of fine and mutually isolated micro-pores, with small pore-throat radii and poor connectivity, resulting in relatively large fluid seepage resistance. Under the action of HPWI, the pore structure of the reservoir undergoes significant reconstruction: on the one hand, the original pore throats are gradually widened due to the scouring and expansion effects of high-pressure fluids, and the increase in pore-throat radii is more obvious in high-permeability layers; on the other hand, the micro-fractures generated during the expansion process are intertwined and connected with the primary pores and pore throats, breaking the originally isolated pore distribution pattern and gradually forming a "pore–micro-fracture" composite connected network, thereby significantly reducing the tortuosity of fluid migration, as shown in Figure 1. Meanwhile, the rearrangement of rock particles caused by the expansion effect further optimizes the distribution of pore space, making the pore size tend to be uniform, reducing the local seepage bottlenecks caused by the non-uniformity of pore structure, and thereby enhancing the overall seepage capacity and fluid migration efficiency of the reservoir.



Figure 1. Schematic diagram of fracture distribution before and after HPWI expansion in Block A. (**a**) The development of natural fractures and micro-fractures in the reservoir; (**b**) high-pressure injection fluid opens natural fractures; (**c**) a large number of micro-fractures are induced. (Blue represents injected water, gray represents natural fractures, and white represents activated natural fractures).

2.2. Numerical Model Building

The core foundation of this model is the mass conservation equation and the Darcy flow equation, which are used to describe the flow and material conservation of oil, water and gas in the equivalent continuous medium. At the same time, a permeability stress-sensitivity function is introduced to quantitatively characterize the dynamic response and property changes in the equivalent matrix (including micro-fracture systems) in the pore structure under high-pressure water injection. By introducing the permeability correction coefficient β_k to represent the sensitivity, the expression method is as follows:

$$\sigma_e = \sigma - \alpha P_p \quad (1)$$

$$K(\sigma_e) = \beta_k K_0 e^{-\alpha_k \sigma_e} \quad (2)$$

where P_p is the pore pressure, MPa; α is the Biot coefficient; σ is the total rock stress, MPa; σ_e is the effective rock stress, MPa; $K(\sigma_e)$ is the rock permeability, in mD; K_0 is the initial permeability, mD; α_k is the permeability stress-sensitivity coefficient, dimensionless; and β_k is the permeability correction coefficient, dimensionless. When $\sigma_e > 0$, the order of magnitude of the stress-sensitivity coefficient α_k is from 10^{-4} to 10^{-3}, and the permeability correction coefficient β_k is 1. When $\sigma_e < 0$, the order of magnitude of the stress-sensitivity coefficient β_k is 10^{-3}, and the permeability correction coefficient β_k is greater than 1.

For the method of explicitly characterizing macroscopic fractures using the Embedded Discrete Fracture Model (EDFM), the Forchheimer's law for non-Darcy high-speed flow of multiphase fluids is followed:

$$\text{Oil}: -(\nabla p_o - \rho_o \nabla D) = \frac{\mu_o}{k_{\text{rf}}} k v_o + \beta_o \rho_o v_o |v_o \tag{3}$$

$$\text{Water}: -(\nabla p_w - \rho_w \nabla D) = \frac{\mu_w}{k_{\text{rf}}} k v_w + \beta_w \rho_w v_w |v_w \tag{4}$$

$$\text{Gas}: -\left(\nabla p_g - \rho_g \nabla D\right) = \frac{\mu_g}{k_{\text{rf}}} k v_g + \beta_g \rho_g v_g |v_g \tag{5}$$

where β is equivalent non-Darcy flow coefficients of oil, water, and gas under multiphase flow conditions, m^{-1}; and the subscript f is the fracture.

The reservoir matrix of each simulation case is treated as equivalent homogeneous at the research scale (porosity, permeability and relative permeability curves are isotropic and do not evolve over time), and fractures are given a preset geometric form (length/complexity is given by the scheme, and fracture width and conductivity are fixed within a single case), while the additional impact of large-scale structural changes between wells on connectivity is ignored; therefore, the differences in results under different working conditions mainly correspond to the changes in the range/morphology of micro-fracture damage and the scale/complexity of macro-fractures.

2.3. Parameter Settings of the Numerical Simulation Model

Based on the physical mechanism of the reservoir and the actual development conditions, this model presupposes a dual-zone structure of "static damage zone + fracture development zone" and constructs a numerical model of the five-spot well pattern with "one injection and four production" to truly reproduce the injection and production development mode of Block A under high-pressure water injection conditions. The core lies in the characterization of the physical, chemical, and mechanical behaviors of the reservoir rocks and fluids in Block A, as well as those in the injection–production process. Compared with empirical models, this model emphasizes strict adherence to actual geological and engineering laws. By introducing physical mechanisms such as porosity, permeability, relative permeability, capillary force, PVT phase change, multiphase flow laws, and wellbore–formation coupling, it can reflect the dynamic response of the reservoir during water injection and high-pressure water injection development processes. Focusing on the core problem of water channeling during HPWI in the ultra-low permeability reservoir of Block A, a precise numerical model is constructed to clarify the action mechanisms of the matrix, micro-fractures, and macro-fractures during the HPWI process. The influence laws of different factors on water channeling are analyzed to provide model support for revealing the formation mechanism of water channeling and formulating prevention and control countermeasures. The specific simulation idea is shown in Figure 2.

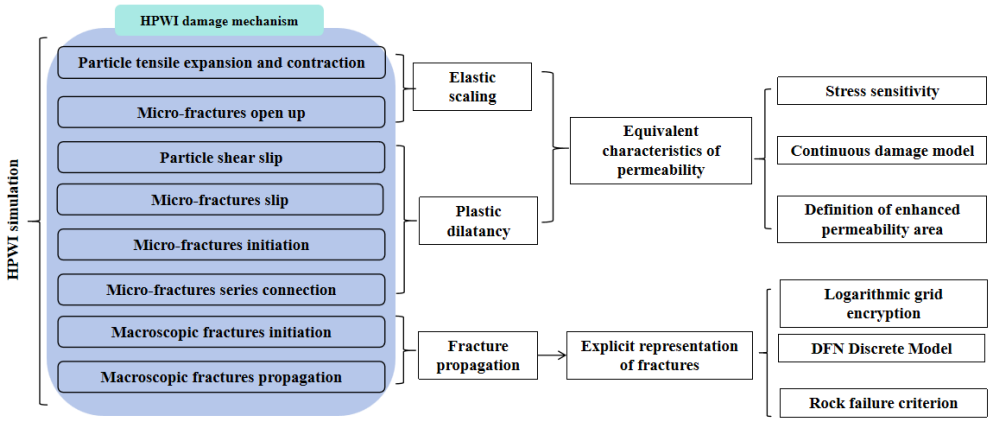


Figure 2. Numerical simulation idea for HPWI.

Modeling and simulation studies were conducted using the numerical simulation software CMG 2024.20. The model size is 1000 m × 1000 m × 10 m, with a Cartesian coordinate grid having a step size of 20 × 20 × 10. The operation model is the black-oil (IMEX) model. The basic information of the simulated reservoir is shown in Table 1. The local permeability correction factor was adjusted through sensitivity analysis in the historical fitting, and the fitting error of the overall recovery degree was controlled within 3%.

Table 1. Basic information of model settings.

Parameter	Value	Unit
Injection–production well spacing	370	m
Top depth	3650	m
Permeability	16.26	mD
Porosity	0.15	/
Initial oil saturation	0.684	/
Formation pressure	22	MPa
Rock compressibility coefficient	7×10^{-7}	kPa^{-1}
Matrix permeability coefficient	0.002	/
Matrix permeability coefficient	1	/
Fracture permeability coefficient	0.007	/
Fracture permeability coefficient	3.0155	/

3. Simulation of the Core Action Mechanism of HPWI

3.1. Micro-Fracture Damage

The influence of micro-fracture damage on water channeling in HPWI has distinct "indirectness" and "staged" characteristics, and its effect depends on the scale of the damage and its relationship with the development degree of macroscopic fractures [28,29]. To quantitatively describe the spatial development characteristics of micro-fracture damage and its impact on seepage response, it is necessary to parameterize the micro-fracture damage from two aspects: the scale of the damaged area and the morphology of the damaged area.

The area of micro-fracture damage refers to the spread range of the micro-fracture concentration development zone on the plane or in space caused by the re-distribution of injection pressure and in situ stress under the effect of HPWI. It is an important quantitative index to describe the degree of micro-fracture damage. Micro-fracture damage does not directly control water channeling under HPWI, but it changes the stress distribution and seepage path of the formation, intensifies the extension trend of the main fractures, and creates conditions for the macroscopic fracture connection. Its influence on water channeling

depends on the cooperative effect of macroscopic fractures. When the macroscopic fractures have not reached the critical length, the influence of micro-fracture damage is limited; once the macroscopic fractures exceed the critical scale, micro-fracture damage will further aggravate the degree of water channeling.

The area of the micro-fracture damage zone is usually characterized by the statistics of the numerical simulation grid; it can also be directly converted based on the planar projection area of the reservoir. In the established mechanism model, the grids of the micro-fracture damage zone were set to 49, 109, 169, 289, and 461 respectively. The variation laws of the formation water saturation and the water cut of the oil well corresponding to different grid counts of the micro-fracture damage zone were analyzed, as shown in Figure 3.

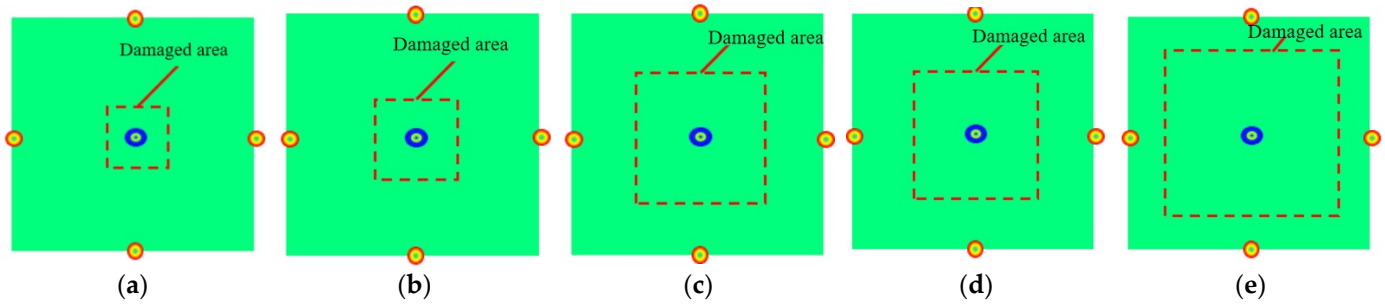


Figure 3. Different micro-fracture damage areas (grid number): (**a**) grid number = 49; (**b**) grid number = 109; (**c**) grid number = 169; (**d**) grid number = 289; and (**e**) grid number = 461.

The shape of the micro-fracture damage zone refers to the geometric distribution characteristics of the damage zone formed in the reservoir due to the concentrated development of micro-fractures during the HPWI in block A. The core evaluation index is the "aspect ratio", which is used to quantitatively reflect the directionality and concentration of micro-fractures [30]. This morphology is determined by the redistribution of strata stress and rock deformation caused by high-pressure water injection, and is jointly controlled by factors such as reservoir heterogeneity, the main direction of in situ stress, and natural fracture systems. Therefore, it shows different extension trends. The aspect ratio is defined as the ratio of the length of the damage area along the main streamline direction to the width perpendicular to the main streamline direction. In the established mechanism model, the aspect ratios of the shape of the micro-fracture damage area are set to 1, 6, and 25 respectively, and the variation laws of the formation water saturation and the water cut of the production well corresponding to different aspect ratios of the micro-fracture damage area are analyzed.

3.2. The Influence of Macro-Fractures on Water Channeling

Under the model settings and the working conditions of Block A in this paper, the macroscopic fracture scale shows the strongest correlation with the water channeling risk and is one of the key factors controlling the transformation of the seepage mode and the channeling intensity. They determine the occurrence conditions and development intensity of water channeling by directly reshaping the seepage pattern and regulating the distribution path of injected water [31,32]. Different scenarios of fracture lengths are constructed through numerical simulation, and the actual fracture scale is inverted by combining with field production performance (such as sudden changes in water cut and pressure response). The critical length of macro-fractures is an important criterion for determining whether water channeling occurs during HPWI. Its control mechanism is mainly composed of two key parameters: fracture length and fracture complexity. The fracture length determines the main seepage medium between injection and production wells and is the core trigger factor

for the initiation of water channeling. Different length intervals correspond to completely different water channeling risks. The fracture complexity affects the advancing speed and diffusion range of channeling flow by changing the distribution pattern of injected water in the fracture network [33,34].

In the established mechanistic model, the lengths of macro-fractures are set to 50 m, 150 m, 200 m, 250 m, and 300 m respectively, and the complexity levels of macro-fractures are set to high and low respectively. Then, the variation laws of the formation water saturation and the water cut of production wells under different fracture lengths and complexity levels are analyzed.

4. Results and Discussion

4.1. Influencing Factors of Water Channeling Formation in HPWI

4.1.1. The Influence of Micro-Fracture Damage on Water Channeling

Micro-fracture damage is a direct result of the process of formation expansion and stress release induced by HPWI, which occurs along with the disturbance of the matrix structure and is mostly distributed near water injection wells and potential main flow lines and dominant seepage zones. The water saturation of the formation corresponding to different micro-fracture damage areas is shown in Figure 4. When the damage area is relatively small (49 grids), it cannot form a clear directional guidance for the main fracture, and the expansion of the main fracture is still controlled by the overall stress field, with no significant change in the water channeling risk. When the damage area is relatively large (461 grids), the equivalent weakened zone corresponds to a stronger directional extension trend of the main crack. As a result, when the macroscopic crack is close to being fully connected, it exhibits a higher risk of water channeling.

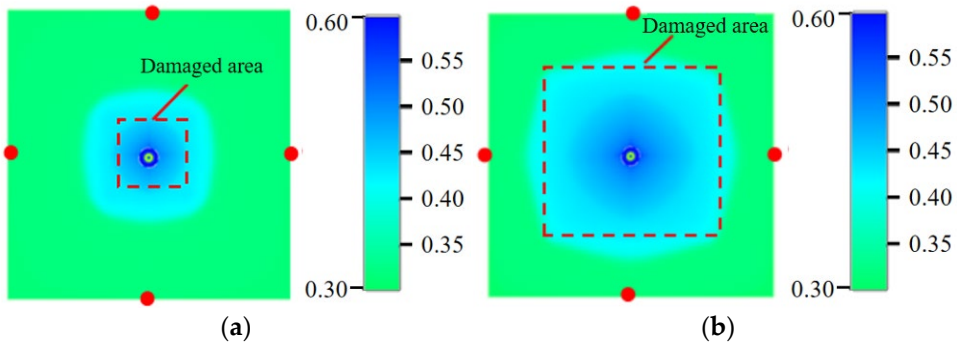


Figure 4. Water saturation of formation corresponding to different micro-fracture damage areas: (**a**) the area of micro-fracture damage is small (grid number = 49); (**b**) the area of micro-fracture damage is large (grid number = 461).

Figure 5 shows the water cut curves of production wells corresponding to different micro-fracture damage zone areas. The micro-fracture damage zones do not directly dominate water channeling, but they will indirectly increase the risk by strengthening the extension trend of the main fractures. When the number of grids in the damaged area is greater than 300, an equivalent weakening zone will form to guide the directional expansion of the main fracture, significantly accelerating the rising rate of the moisture content. When the number of grids is less than 200, the guiding effect on the main fracture is weak, and the risk of water channeling is controllable. When the damaged area is small (e.g., 49 grids), the water cut remains at a low level for a long time and rises gently. The water cut is still below 0.4 in the later stage of production, showing no obvious signs of water channeling. When the damaged area is medium (e.g., 100, 169, 289 grids), the rising rate of the water cut gradually increases with the increase in the number of grids, and the slope of the curve increases, which reflects the gradual enhancement of the water channeling risk due to the expansion of the damaged

area. When the damaged area is large (e.g., 461 grids), the water cut rises the fastest, quickly exceeding 0.5 in the early stage and approaching 0.7 in the later stage of production. The risk of water channeling is significantly higher than that of other groups.

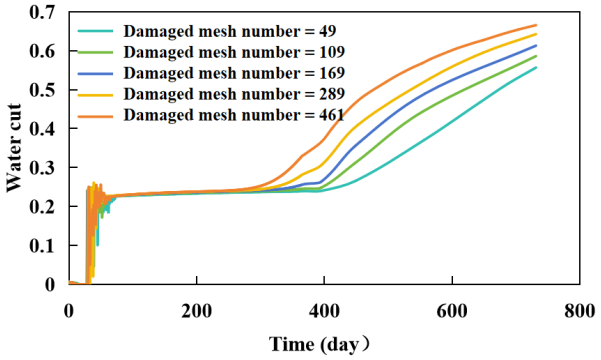


Figure 5. Water cut curves of production wells corresponding to different areas of micro-fracture damage zones.

In addition, Figure 5 also shows that the moisture content remains basically stable between 0.20 and 0.23 from 0 to 300 days, hardly affected by the damaged area of micro-cracks. After 400 days, the differences among different damaged area conditions gradually emerge: when the number of damaged grids is 49, the moisture contents at 400, 600, and 750 days are approximately 0.30, 0.42, and 0.48 respectively; when the number of damaged grids increases to 461, the moisture contents at the same periods rise to about 0.40, 0.61, and 0.67. Correspondingly, the average rising rate of the moisture content from 400 to 750 days increases from about 0.00051 d^{-1} to about 0.00074 d^{-1}, with an increase of about 45%. When the number of damaged grids exceeds about 300, the moisture content exceeds 0.5 around 450 days and approaches 0.7 at the end of production. This indicates that after the formation of an equivalent weakened zone in the micro-crack-damaged area, the directional extension of the main crack and the risk of water channeling are significantly enhanced. Therefore, a grid number exceeding 300 is an important risk threshold that requires key attention.

Similarly, the formation water saturation corresponding to different micro-fracture damage shapes is shown in Figure 6. When the damage is uniformly distributed (aspect ratio = 1), the injected water displaces uniformly, the water cut rises slowly, and the inducing effect on water channeling is extremely weak. When the damage has a strong directivity (aspect ratio = 25), although secondary seepage channels may be formed, the growth of water cut slows down in the high-water-cut period. It is difficult to form high-permeability channels in a short time only based on the geometric shape, and macroscopic fractures need to be superimposed to enhance the channeling velocity.

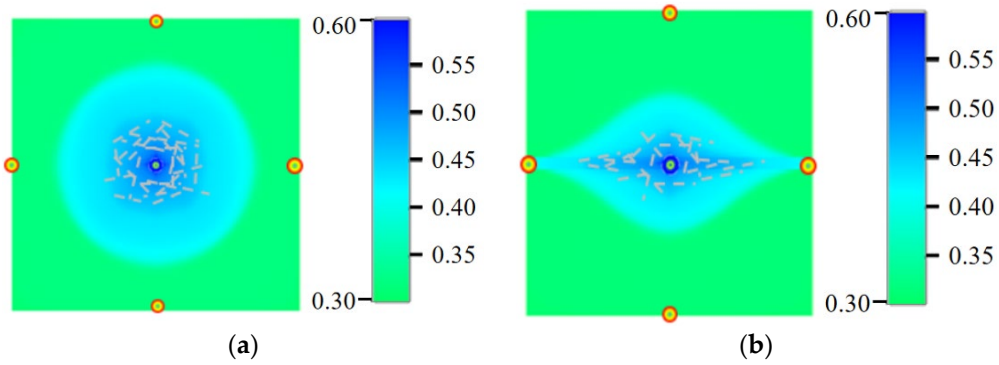


Figure 6. Water saturation of formation corresponding to different shapes of micro-fracture damage: (**a**) shape of the micro-fracture damage area (aspect ratio = 1); and (**b**) shape of the micro-fracture damage area (aspect ratio = 25).

Comparing the water cut curves of production wells under different shapes of micro-fracture damage areas (Figure 7), the water cut remains at a relatively low level when the aspect ratio is 1 or 6, while it is significantly higher when the aspect ratio is 25. When the aspect ratio is 1, the water cut rises most gently, remaining stable in the range of 0.3–0.6 throughout the process. It is still below 0.6 in the later stage of production, showing no obvious signs of water channeling. When the aspect ratio is 6, the increased rate of water cut is slightly higher than that when the aspect ratio is 1. Overall, it is in the range of 0.3–0.7. The growth rate slows down during the high water cut period, and there is no rapid and sudden increase. When the aspect ratio is 25, the rising rate of water cut is the fastest. It breaks through 0.5 in the early stage and approaches 0.9 in the later production stage. The risk of water channeling is much higher than in the previous two cases.

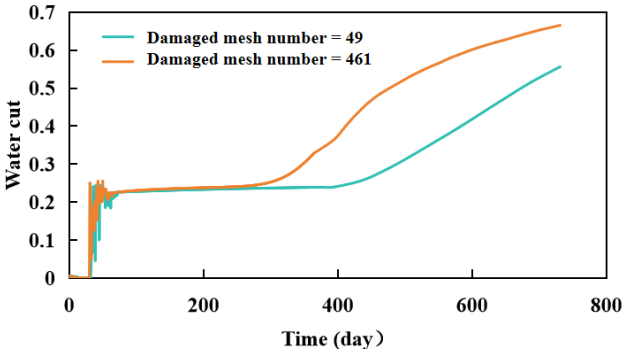


Figure 7. Water cut curves of production wells under different shapes of micro-fracture damage zones.

Physically, the observed increase in water cut is a direct consequence of how HPWI reshapes the local pressure field and flow pathways. At the early stage of injection, the pressure gradient between injector and producer is relatively uniform, and the injected water front advances mainly through the matrix with only limited influence from existing micro-fractures. As injection pressure increases, the pressure gradient becomes concentrated along vulnerable directions where micro-fracture networks and pre-existing weakness planes exist. This induces local permeability enhancement or damage, which in turn redistributes the effective transmissibility field. The flow paths are gradually reorganized from a dispersed pattern into preferential corridors with lower flow resistance. Once a high-conductivity macro-fracture or a connected micro-fracture belt is established between the wells, the majority of the injected water is diverted into this short-circuit channel, sharply increasing the water saturation near the producer and leading to the rapid rise in water cut.

4.1.2. The Influence of Macro-Fractures on Water Channeling

The characteristics of water saturation corresponding to the critical fracture half-length without channeling and the fracture half-length with channeling are shown in Figure 8. From the water saturation image corresponding to the critical fracture half-length without channeling (200 m) (Figure 8a), it can be seen that the curve is gentle without a sudden upward trend. At this time, the seepage mode is in the transition stage from "fracture + matrix" to "fracture-dominated". The injected water has not formed a through-going channeling path. The displacement process is relatively balanced, and there are no obvious signs of water flooding in the production wells. This clearly indicates that this half-fracture length is the critical boundary for water breakthrough. In contrast, when the fracture half-length in Figure 8b increases to 250 m, the water saturation image shows a sharp upward trend, and the water saturation rapidly approaches a high value. At this stage, the seepage mode has completely transformed into being controlled by the "main fracture", and a high-conductivity channel for cross-flow is formed between the injection

and production wells. The injected water quickly breaks through to the production well, resulting in significant water flooding of the production well in a short period of time. This directly reflects the explosive growth of water channeling risk when the half-fracture length exceeds the critical value.

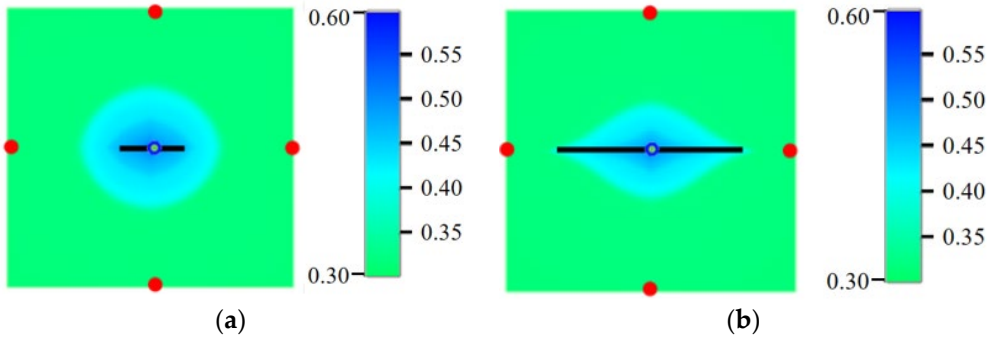


Figure 8. Water saturation of formation corresponding to different fracture half-length: (**a**) critical fracture half-length without channeling (200 m); and (**b**) half-length of the channeling fracture (250 m).

The water cut curves of the production wells under different fracture half-lengths are shown in Figure 9. The half-length of fractures has a significant control effect on the seepage pattern of the reservoir and water channeling behavior. When the fracture half-length is less than 150 m, the seepage in the reservoir is still dominated by the "matrix + fracture" cooperative effect. Although the injected water achieves rapid energy transfer within the fractures, its diffusion into the matrix is relatively slow, and the displacement process is stable. The water cut curve shows no significant anomalies, the production wells are affected evenly, and water channeling characteristics are basically not exhibited. When the fracture half-length is within the range of 150–200 m, the seepage pattern enters a transitional stage where it shifts from "fracture + matrix" to "fracture-dominated". At this point, the flow-conducting advantage of the fractures gradually becomes apparent, and the advancing speed of the injected water along the fractures significantly increases, but a completely connected water channel has not yet formed. Some production wells may show a slow increase in water cut, but the overall situation has not yet reached a severely water-flooding state. When the fracture half-length is greater than or equal to 250 m, the seepage mode is completely evolved into the "dominant fracture control" mode. The fractures connect the injection and production wells, forming high-conductivity channeling paths. The injected water breaks through almost rapidly along the dominant fractures, resulting in a sharp water breakthrough in the production wells in a short period. For example, under this fracture length condition, the water cut of well x51 rapidly increased from 10.3% to 93.6% within 3 days, forcing the well to shut down. Overall, under the numerical simulation and field conditions of Block A in Oilfield S in this study, when the fracture half-length reaches approximately 70% of the well spacing between injection and production wells (about 259 m), the risk of water channeling shows an exponential upward trend. This ratio can be used as a critical criterion for the occurrence of water channeling under high-pressure water injection conditions and has significant practical warning significance.

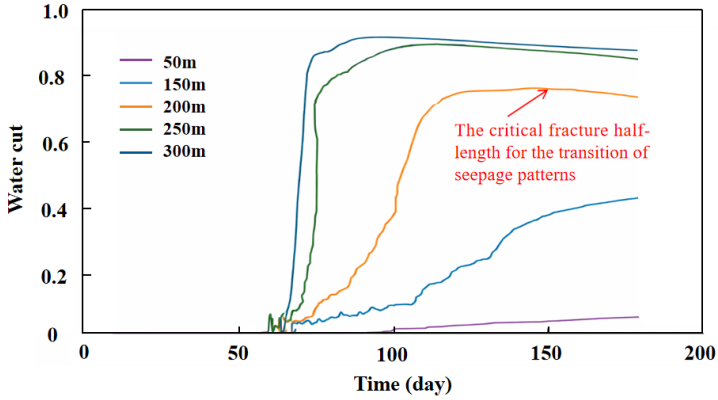


Figure 9. Water cut curves of production wells under different half-lengths of fractures.

Similarly, from the distribution of formation water saturation corresponding to different fracture complexities, it can be seen that when the fracture complexity is relatively high, the fracture network exhibits the characteristics of multiple branches and cross-connections. The multi-branch structure can effectively disperse the injected water flow and prevent the water from advancing concentratedly along a single channel (Figure 10a). The injected water is evenly distributed in the fracture network, with a wider displacement range. Each area of the reservoir is affected evenly, and no high-conductivity channeling channels are formed. Therefore, the water saturation rises slowly, and the risk of water channeling is low, which reflects the mitigation effect of the complex fracture network on water channeling. On the contrary, as shown in Figure 10b, when the complexity of fractures is relatively low, there is mainly a single dominant fracture in the reservoir, without obvious branching or intersecting structures. The injected water lacks diversion paths and can only advance rapidly along the dominant fracture. The dominant fracture becomes the only high-conductivity channel, with a fast water breakthrough speed. It is easy to form a through-flow channel between the injection and production wells, resulting in significant water flooding of production wells in a short period.

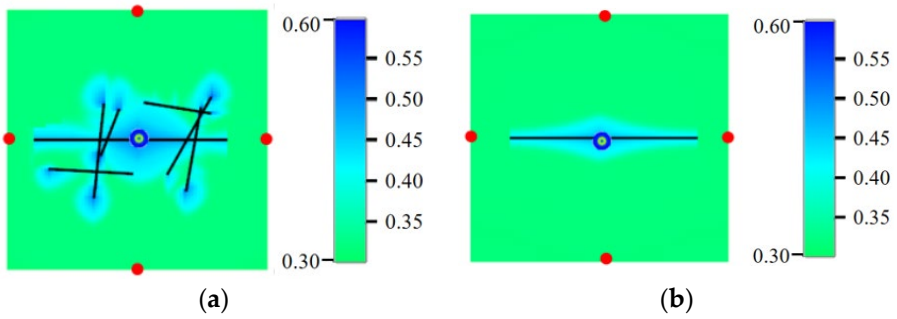


Figure 10. Water saturation of the formation corresponding to different degrees of fracture complexity: (**a**) high complexity of fractures; and (**b**) low complexity of fractures.

From the variation curves of production well water cut under different fracture complexity conditions (Figure 11), it can be seen that the fracture complexity significantly affects the advancing speed and spatial expansion range of water channeling by adjusting the distribution mode of injected water in the fracture network. Its action mechanism shows an obvious synergistic relationship with the fracture length. When the complexity of fractures is relatively low (mainly featuring a single main fracture), the injected water mainly advances in a concentrated manner along the single main fracture. It has a weak diversion ability, with the channel conductivity highly concentrated. The water breakthrough speed is fast, and the risk of water channeling is concentrated and intense. This type of

fracture morphology can easily lead to the rapid water flooding of production wells in the direction of the main streamline in a short period of time. When the complexity of fractures is relatively high (manifested as multi-branched or intersecting fracture networks), multi-branched fractures can effectively disperse the flow of injected water, allowing it to spread along multiple paths. This weakens the flow-guiding advantage of a single main channel, delays the formation of the dominant channel, and reduces the water breakthrough velocity, thereby weakening the risk of water channeling to a certain extent. At this time, the sweep area of the injected water is significantly expanded, the production wells respond more evenly, and the increase in water cut is relatively gentle.

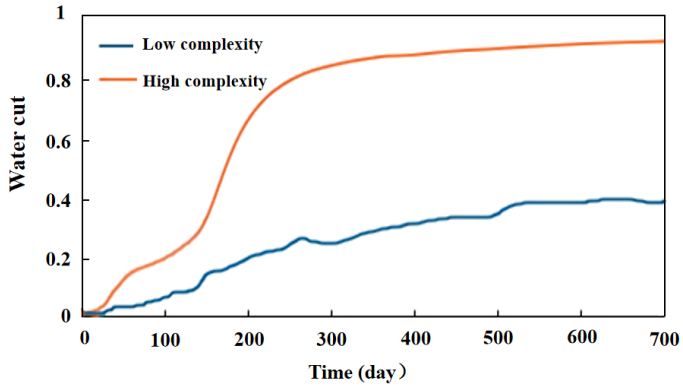


Figure 11. Water cut curves of production wells under different degrees of fracture complexity.

4.2. The Key Mechanism of Water Channeling Formation

Based on the sensitivity results in Section 4.1, this section summarizes and explains the above phenomena from the perspective of the evolution of seepage patterns. The differences among the simulated channeling scenarios can be interpreted in terms of three coupled physical processes: pressure-field evolution, permeability redistribution, and fracture conductivity variation. First, HPWI generates a strong pressure disturbance around the injector, and the resulting pressure gradient governs the direction and rate of water advance. As fractures grow or become reactivated, the pressure field is progressively focused along these high-conductivity paths. Second, micro-fracture damage locally alters the rock fabric, which is reflected in the model as a spatial redistribution of effective permeability. Depending on the extent and aspect ratio of the damaged zone, this can either create a broad, low-contrast conductivity region that promotes distributed sweep, or form a narrow weakened belt that guides the main fracture towards the producer. Third, the conductivity of macro-fractures controls how much of the injected water bypasses the matrix. As fracture length and complexity evolve, the fracture network may either support cooperative fracture–matrix flow, or develop into a dominant short-circuit conduit with high mobility contrast to the surrounding rock.

From Section 4.1, it is known that the core mechanism of water channeling formation is the transformation of the injection water seepage mode. During this process, the macro-fracture expansion scale (especially when the fracture half-length is $\geq$70% of the injection–production well spacing) is the direct determining factor leading to water channeling. The damage geometric characteristics of micro-fractures indirectly affect the risk of water channeling by strengthening the extension trend of the main fractures, which is manifested macroscopically as an imbalance in the swept volume and intensified channeling flow. These two types of factors jointly regulate the formation of water channeling, among which the macroscopic fracture expansion scale plays a dominant role.

The “fracture + matrix” seepage is the main seepage mode in the early stage of high-pressure water injection development, as shown in Figure 12a. Its essence is a synergistic

process in which fractures and the matrix jointly participate in fluid migration. The displacement process is relatively gentle and balanced, and there is basically no risk of breakthrough water channeling. In this mode, the micro-fracture network and matrix pores together form a dual-channel system: the fractures undertake the functions of rapid energy transfer and initial water-phase advancement, while the matrix serves as the main crude oil reservoir and the main area for water flooding. At this time, the injected water advances in a dispersed manner between the fractures and the matrix, and no clear dominant seepage path is formed. The energy of high-pressure water injection is first rapidly transmitted within the fracture system and then diffuses into the surrounding matrix pores at a lower speed, achieving a coupling effect of "rapid energy transfer–slow displacement". Since the distribution of energy and water flow in space is relatively uniform, all areas of the reservoir can be swept to a certain extent, without local energy concentration or channelized flow. Therefore, the overall displacement process is stable, which is beneficial to improving the volume utilization degree and maintaining the controllability of the injection–production relationship.

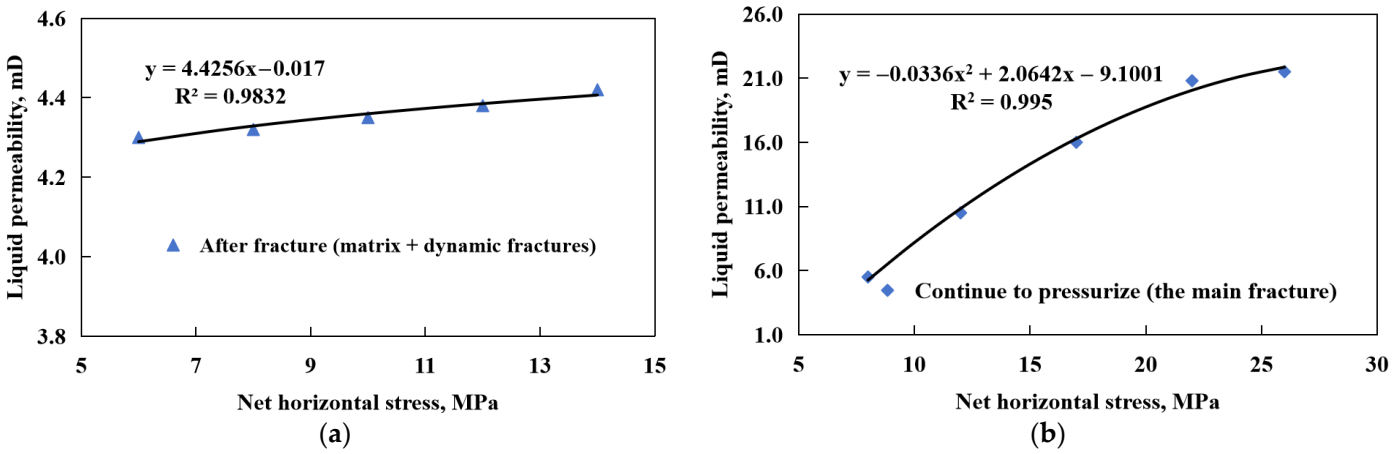


Figure 12. Seepage modes at different stages of high-pressure water injection: (**a**) "fracture + matrix" seepage mode; and (**b**) "main fracture" seepage mode.

As the water injection continues, when the macro-fractures further expand and connect between wells, as shown in Figure 12b, the seepage pattern gradually evolves into the late-dominant pattern characterized by "main fracture control". At this time, the connected macroscopic main fractures become almost the only fluid migration channels. The displacement process shows significant centralization and breakthrough, which is the direct cause of water channeling. Under this pattern, the macroscopic main fractures completely dominate the seepage process. The participation of matrix pores in water flooding is significantly reduced, and they hardly undertake the effective fluid transport function. The injected water forms highly fixed "short-circuit channels" along the connected main fractures. The flow path is single and the resistance is extremely low, resulting in the extreme spatial concentration of high-pressure water injection energy. Although the energy transfer speed is extremely fast, it is difficult to effectively diffuse to the surrounding matrix. Eventually, a breakthrough-type displacement pattern of "high energy, high speed, and narrow range" is formed. Once the main fractures connect the injection and production wells, the water flow will rapidly break through to the production well in a very short time, inducing sudden water flooding, which marks the occurrence of water channeling.

After the seepage mode changes, the injected water no longer advances uniformly through the reservoir. Instead, it forms preferential channels along the main fractures and finger-fronts rapidly. This causes the water saturation in the high-permeability fractures

to rise rapidly, while the surrounding matrix and low-permeability areas remain in an ineffective displacement state, presenting a typical non-equilibrium displacement pattern of "locally high water cut and globally low utilization". The fundamental reason is that after the fractures penetrate the high-permeability layer, the capillary force's constraint on the water phase is significantly weakened. The injected water tends to flow concentratedly along the main fractures with the least resistance, thus completely changing the original volume sweep path. This shift in the sweep volume further amplifies the channeling behavior, manifested as abnormal dynamics such as a sharp increase in the water cut of production wells, a rapid decline in daily oil production, and a significant rise in the dynamic fluid level. Meanwhile, the high conductivity of the main fractures allows the subsequent injected water to continuously converge in the dominant channels, strengthening the positive feedback effect of "the more it channels, the more permeable it becomes; the more permeable it becomes, the more it channels", and the channeling speed keeps accelerating. Eventually, it not only causes individual wells to be flooded prematurely and even shut down but also undermines the energy utilization efficiency of high-pressure water injection in the entire well group, exacerbating the waste of formation energy and resulting in a loss of recovery factor.

4.3. Mainstream Regulation Technology

4.3.1. Selection of Pilot Demonstration Well Groups

Based on the effectiveness of high-pressure water injection well groups in Block A of Oilfield S and the production characteristics of the block, the spatial distribution and flow control intensity of the dominant channeling channels in each well group, as well as their response relationship with the production performance, were determined [35]. The well groups in Block A of S Oilfield are classified into two types: ① high-risk water channeling well groups (with equivalent half-fracture length $\geq$ 70% of well spacing and the number of grids in the micro-fracture damage zone > 300), and ② medium–low-risk well groups (with half-fracture length < 70% of well spacing and the number of grids in the micro-fracture damage zone < 200). For the medium–low-risk well groups, the "soft regulation" approach is mainly implemented through optimizing the injection and production system and periodic water injection. For the high-risk well groups, the combination of "chemical profile control and periodic water injection" is prioritized as a strong control solution.

The development effect of well group x41 is characterized by high water cut, low oil increment, and strong heterogeneity. During the HPWI period, the production carried out simultaneously causes the injected water to break through rapidly along the high-permeability layers. The comprehensive water cut is 70.3%, with three water-channeling wells, and the cumulative oil increment is only 130 tons. The identification of dominant channels (Figure 13) shows that the half-length of the dominant channels in well group x41 is greater than 250 m, approaching 70% of the well spacing. This is consistent/corresponds with the dynamic situation where the water cut of well 51 increased rapidly in the short term, triggering a sudden water breakthrough in well 51 within 3 days. Moreover, there is a large-scale micro-fracture damage weakening zone in the direction of the main streamline, which meets the "high-risk working conditions". Therefore, well group x41 was selected as the priority pilot demonstration well group.

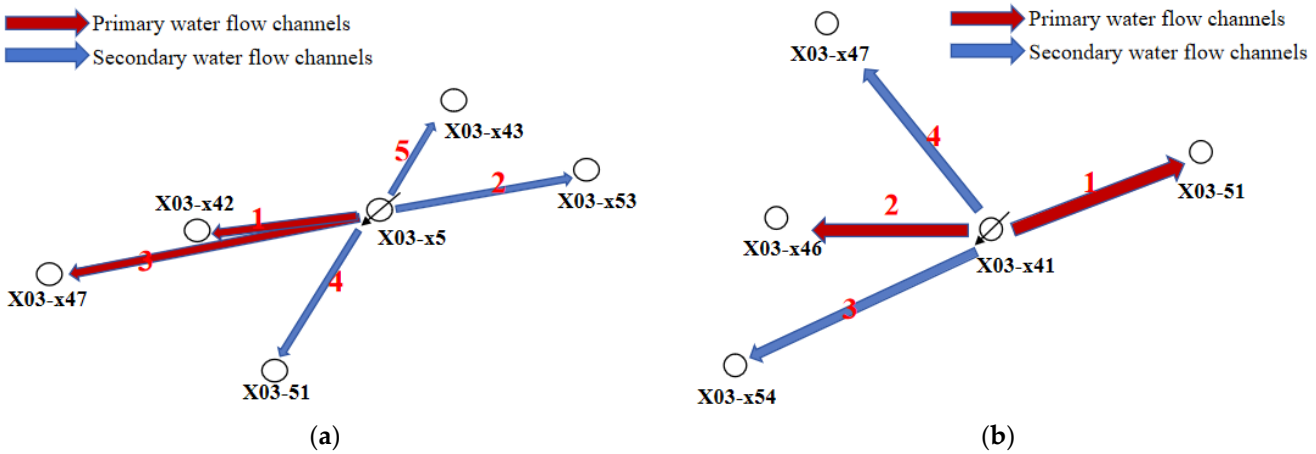


Figure 13. Distribution results of dominant flow channels in full small layers of different well groups: (**a**) well group x5; and (**b**) well group x41. The red numbers sorting represents the order of effectiveness from first to last.

4.3.2. Performance Adaptability Analysis of the Profile Control System for Well Groups

In order to systematically screen and optimize the profile control system suitable for the high-temperature, high-salinity and low-permeability reservoir conditions of Block A in Oilfield S, this paper designs and develops a water-based self-assembling microsphere profile control and plugging agent. During the self-assembly process, these microspheres can form visible micelles or network-like aggregated structures by the naked eye, thus significantly enhancing the plugging ability of reservoir pore throats. To balance good injectability and plugging effects, microspheres with an average particle size of 200 nm are selected as the main body for profile control and plugging. The specific formula consists of nonionic polymer protective colloid (0.5 wt%), slow-release crosslinking agent (0.2 wt%), and high-temperature resistant stabilizer (0.1 wt%). The evaluation results of the plugging performance (Table 2) show that the plugging rate of this profile control agent decreased by less than 0.3% after 120 days of aging. After being flushed with 50 PV of standard brine, the plugging rate only dropped by 2.31%. The above results indicate that the water-based self-assembled microsphere profile control agent has excellent sealing stability and long-term erosion resistance, which can meet the profile control application requirements under the reservoir conditions of the block.

Table 2. Evaluation of the plugging performance of the profile control system.

No	$K_1/\times10^{-3}$ μm^2	H/%	Percentage Decrease in Plugging Rate at Different Aging Times/%			
			30 d	60 d	90 d	120 d
1	118.4	93.12	0.02	0.03	0.06	0.09
2	188.8	90.40	0.03	0.08	0.11	0.14
3	285.1	87.34	0.05	0.09	0.12	0.14
4	368.4	83.49	0.03	0.10	0.14	0.19
5	460.9	79.17	0.05	0.11	0.14	0.18

5. Design and Effect Simulation of Mainstream Line Regulation and Control Schemes

The comparison results of the schemes are consistent with the mechanism of the dominant channel control revealed in Sections 4.1 and 4.2. To verify the applicability and effectiveness of the combined regulation strategy of "chemical profile control + cyclic water injection" in a specific well group, targeted program design and numerical simulation

were carried out with the x41 demonstration well group as the object. Combined with Section 4.3, the paper designed and compared two regulation programs: Scheme One is simple cyclic water injection; and Scheme Two is a combined measure of "chemical profile control + cyclic water injection". In view of the seepage characteristics of the target well group, a two-stage alternating cyclic water injection with high and low pressures is adopted. The high-pressure stage lasts for 24–48 h, and the low-pressure stage also lasts for 24–48 h. The total duration of a complete cycle is 2–4 days. Single regulation shall be continuously carried out for 3–6 cycles, and real-time optimization and adjustment shall be made in combination with the fluid production dynamics.

Before the application, the pressure drop of each branch was mainly controlled by the original well pattern/boundary conditions, and the pressure field presented a relatively stable distribution pattern. A "priority flow channel" was formed between the high-pressure and the low-pressure area. After the implementation of the measures, the local boundary conditions changed, resulting in a redistribution of pressure near the wellbore and in the channel area. Some of the original priority channels had a reduced pressure drop and a lower streamline density, while the areas previously limited by insufficient pressure difference gained a larger effective pressure difference and the streamlines migrated towards them. Eventually, under the new pressure equilibrium, the main flow was deflected. The streamline changes in this well group before and after adjustment are shown in Figure 14. After simply implementing cyclic water injection, the flow field is adjusted to a certain extent, and the directions of the main streamlines are somewhat dispersed. However, the influence of the high-permeability channel in the "x41→51" direction is still significant, and the adjustment effect is limited. The improvement effect of the flow field is more significant after adopting the combined scheme (chemical profile control first, followed by periodic water injection). The chemical profile control agent first carried out local plugging on the high-permeability strip in the "x41→51" direction, effectively reducing the flow conductivity of this channel. Subsequently, the optimized cyclic water injection was implemented, which utilized pressure fluctuations to direct more fluid to the areas that had not been affected or were poorly affected previously. The simulated streamline diagram shows that after the implementation of the combined measures, the main streamline is no longer a single strong dominant channel, but a more balanced and multi-directional flow field distribution is formed, and the swept volume is significantly expanded.

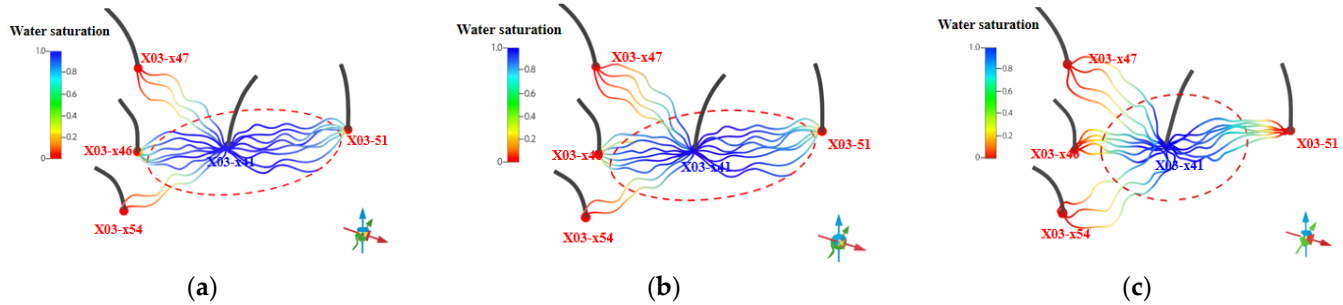


Figure 14. Streamline changes before and after adjustment of well group x41: (**a**) before adjustment; (**b**) after cyclic water injection; and (**c**) after chemical profile control and cyclic water injection.

The simulation results show that the combined scheme reduces the mainstream line contribution rate from 60% to 52% (a decrease of 6%), while the sweep efficiency increases by 5%. By tracking the field application, after the profile control measures were implemented, the daily oil increment of the well group was remarkable. A total of 100 tons of additional oil had been produced during the test period. Based on the crude oil price of 0.235 million yuan per ton in Block A of Oilfield S and the construction cost of 220,000 yuan per well,

the expected input–output ratio is 1:2.1. It should be noted that the comparison of relevant indicators is the estimated result under the scenario of representative well groups, and it is not equivalent to the overall economic conclusion at the block scale for the time being. Overall, this combined strategy has significantly improved the heterogeneous seepage field dominated by high-permeability channels, enhanced the profile control and water shutoff effect as well as the oil displacement efficiency, verified its applicability and application prospects in the x41 demonstration well group, and provided a technical reference for the efficient development of similar complex oil reservoirs.

6. Conclusions

This paper addresses the core challenges of water channeling formation and control in HPWI in low-permeability oil reservoirs. Through geological–engineering coupling modeling, mechanism numerical simulation, and control strategy design, it systematically reveals the main causes of water channeling formation and its evolution laws, and proposes an active control strategy based on the reconstruction of the seepage field. The main conclusions are as follows:

(1) Water channeling under high-pressure water injection in low-permeability reservoirs is not caused by a single factor, but is the result of a coupled process of "pressure-driven fracture evolution–seepage field reconstruction". That is, under the combined action of high-pressure differential drive and reservoir heterogeneity, the multi-scale fracture system reconstructs the seepage resistance field. The mainstream lines evolve from a dispersed type to a concentrated type, and finally an inter-well short-circuit channel is formed, leading to a significant decrease in the volumetric sweep efficiency and a sudden increase in water cut.

(2) The control of micro-fracture damage on water channeling shows significant indirectness and threshold characteristics. Micro-fracture damage itself does not necessarily lead to interwell connection. However, when the damage scope expands or the directionality is enhanced, an equivalent weakening zone will be formed and the local stress–seepage coupling response will be changed. As a result, it will strengthen the directional extension and connectivity of the macroscopic main fractures, indirectly increasing the risk of water channeling.

(3) Macro-fractures are the main controlling factor for water channeling, and there is a clear geometric scale criticality. Numerical results show that when the half-length of the fracture increases from less than 150 m to the range of 150–200 m, the seepage mode is in the transition stage from "fracture–matrix synergy" to "fracture-dominated". When the half-length of the fracture further increases to about 250 m or more, a high-conductivity channel between wells is rapidly established, and the water cut of the production well shows a leap characteristic. Through comprehensive analysis, "the half-length of the fracture reaching about 70% of the injection–production well spacing" can be used as an important critical criterion and early warning indicator for the outbreak of water channeling risk under high-pressure water injection conditions.

(4) The combined strategy of "chemical profile control + cyclic water injection" can reduce the equivalent permeability of preferential channels. By combining with pressure fluctuations, it promotes the redistribution of streamlines, transforming the main streamlines from being "controlled by a single strong channel" to "synergistic displacement through multiple channels", thus realizing the reconstruction of the seepage field and the expansion of the swept volume.

(5) The paper not only provides a theoretical basis and practical guidance for the prevention and control of water channeling in HPWI development of low permeability reservoirs, but also lays a foundation for future research in related fields. Subsequent

research should further explore regulation strategies under different geological conditions to achieve wider application and promotion.

Author Contributions: K.Y. and H.X.: writing—original draft, methodology, investigation, and formal analysis. J.L. and J.W.: writing—review and editing and conceptualization. Z.C. and H.J.: investigation. All authors have read and agreed to the published version of the manuscript.

Funding: This research was funded by the Open Fund of Hubei Key Laboratory of Oil and Gas Drilling and Production Engineering (Yangtze University) (No. YQZC202401) and National Science and Technology Major Project of China (No. 2025ZD1404305, 2025ZD1406103, and 2025ZD1406402).

Data Availability Statement: The original contributions presented in the study are included in the article. Further inquiries can be directed at the corresponding author.

Conflicts of Interest: The authors declare no conflicts of interest.

References

1. Zhang, B. Study on Numerical Simulation of Reservoir Fine Water Injection Development Considering Reservoir Heterogeneity. *Int. J. Energy* **2025**, *6*, 65–68. [CrossRef]
2. Yu, L.; Fei, S.; Zhao, C.; Chen, G.; Cui, Y. Optimal selection of favorable production areas for low-permeability sandstone gas reservoirs in the Benxi Formation of the Upper Carboniferous in Ordos Basin. *Unconv. Resour.* **2025**, *7*, 100134. [CrossRef]
3. Cheng, Q.; Bu, R.; Wei, J.; Zhou, X.; Bai, Y.; Li, J.; Cao, J. Seepage Mechanism and Formation Applicability of Fracture-Assisted Waterflooding Technology in Low Permeability Reservoirs. *Geoenergy Sci. Eng.* **2026**, *258*, 214336. [CrossRef]
4. Ji, B.; Fang, J. An overview of efficient development practices at low permeability sandstone reservoirs in China. *Energy Geosci.* **2023**, *4*, 100179. [CrossRef]
5. He, Y.; Wang, F.; Zhu, J.; Zhou, J.; Chen, S.; Fu, X.; Yang, Y. The research on water control and oil stabilization technologies in ultra-low permeability reservoirs of the Jiyuan oilfield under the control of reservoir architecture. *Sci. Rep.* **2025**, *15*, 4442. [CrossRef] [PubMed]
6. Dong, L.; Zhong, P.; Zhang, Q.; Wang, M.; Dong, W.; Wang, Y.; Yang, C. Experimental Investigation on Layer Subdivision Water Injection in Multilayer Heterogeneous Reservoirs. *ACS Omega* **2023**, *8*, 43546–43555. [CrossRef]
7. Li, X.; Yang, Z.; Li, S.; Huang, W.; Zhan, J.; Lin, W. Reservoir characteristics and effective development technology in typical low-permeability to ultralow-permeability reservoirs of China National Petroleum Corporation. *Energy Explor. Exploit.* **2021**, *39*, 1713–1726. [CrossRef]
8. Chen, L.; Jia, C.; Zhang, R.; Yue, P.; Jiang, X.; Wang, J.; Su, Z.; Xiao, Y.; Lv, Y. High-pressure capacity expansion and water injection mechanism and indicator curve model for fractured-vuggy carbonate reservoirs. *Petroleum* **2024**, *10*, 511–519. [CrossRef]
9. Liu, Y.; Yoshioka, K.; You, T.; Li, H.; Zhang, F. Thermally induced fracture modeling during a long-term water injection. *Int. J. Rock Mech. Min. Sci.* **2025**, *186*, 106022. [CrossRef]
10. Ma, X.; Li, H.; Luo, H.; Nie, S.; Gao, S.; Zhang, Q.; Yuan, F.; Ai, W. Research on well selection method for high-pressure water injection in fractured-vuggy carbonate reservoirs in Tahe oilfield. *J. Pet. Sci. Eng.* **2022**, *214*, 110477. [CrossRef]
11. Cui, C.; Li, H.; Wu, Z.; Zhang, C.; Li, H.; Zhang, Y.; Zheng, W. Analysis of pressures in water injection wells considering fracture influence induced by pressure-drive water injection. *Pet. Reserv. Eval. Dev.* **2023**, *13*, 686–694. [CrossRef]
12. Rudyk, S.; Al-Musalhi, M.; Taura, U.; Spirov, P. Matching of Water Breakthroughs in a Low-Resistivity Oil Reservoir Using Permeability Anisotropy. *Appl. Sci.* **2024**, *14*, 4618. [CrossRef]
13. Li, P.; Liu, Z.; Cai, L.; Chen, Y. The research on high efficiency water injection development of carbonate rock reservoir in the middle east. *Front. Energy Res.* **2024**, *12*, 1396480. [CrossRef]
14. Kong, D.; Peng, Y.; Zhou, Z.; Peng, H.; Chen, Z. Pore-scale mechanism of coupled pressure-driven flow and spontaneous imbibition in porous media during high-pressure water injection processes. *Capillarity* **2024**, *13*, 29–36. [CrossRef]
15. Lei, Z.; Wang, Z.; Mu, L.; Peng, H.; Li, X.; Bai, X.; Tao, Z.; Li, H.; Peng, Y. A technique for enhancing tight oil recovery by multi-field reconstruction and combined displacement and imbibition. *Pet. Explor. Dev.* **2024**, *51*, 152–163. [CrossRef]
16. Zhu, W.; Gao, Y.; Wang, Y.; Liu, P.; Liu, Y. The injection capacity evaluation of high-pressure water injection in low permeability reservoir: Numerical and case study. *Front. Earth Sci.* **2024**, *12*, 1411451. [CrossRef]
17. Li, Y.; Xu, H.; Fu, S.; Zhao, H.; Chen, Z.; Bai, X.; Li, J.; Xiu, C.; Zhang, L.; Wang, J. Analysis of the effectiveness mechanism and research on key influencing factors of high-pressure water injection in low-permeability reservoirs. *Processes* **2025**, *13*, 2664. [CrossRef]
18. Li, M.; Qu, Z.; Wang, M.; Ruan, W. The influence of micro-heterogeneity on water injection development in low-permeability sandstone oil reservoirs. *Minerals* **2023**, *13*, 1533. [CrossRef]

19. Zhang, Y.; Gai, C.; Song, B.; Jiang, J.; Wang, Z. The influence of permeability and heterogeneity on chemical flooding efficiency and remaining oil distribution—Based on NMR displacement imaging. *Sci. Rep.* **2023**, *13*, 14316. [CrossRef]
20. Cao, X.; Liu, H.; Ren, Y.; Jia, Y.; Niu, X.; Sun, C. Progress and prospects of development technologies for lowpermeability oil reservoirs in Shengli Oilfield. *Pet. Geol. Recovery Effic.* **2024**, *31*, 48–55.
21. Liu, J.; Jin, Z.; Cai, X. Streamline influencing factor analysis and its application of streamline adjustment in fault block oil reservoir. *Reserv. Eval. Dev.* **2019**, *9*, 24–29. [CrossRef]
22. Shu, N.; Liu, L.; Yao, X.; Huang, Y.; Lai, F.; Cui, W. Formation mechanism of extreme water consumption zone and synergistic mode of flow field regulation: A case study of uncompartmentalized oilfield of continental sandstone in the late stage of ultra-high water cut. *Pet. Reserv. Eval. Dev.* **2024**, *14*, 237–246. [CrossRef]
23. Kazem, M.H.; Hussein, M.A.; Adnan, M.S.; Alfarge, D.; Mansour, I.J. The performance of streamline simulation technique to mimic the waterflooding management process in oil reservoirs. *Fuel* **2023**, *348*, 128556. [CrossRef]
24. Zhang, L.; Li, Y.; Song, X.; Hu, D.; Yu, Y.; Zhao, Z.; Wang, W.; Liu, C.; Lv, M. A streamline-based production optimization method for waterflooding reservoirs. *Sci. Rep.* **2025**, *15*, 37569. [CrossRef] [PubMed]
25. Yin, H.; Yu, J.; Qu, H.; Yin, S. A Novel Approach to Waterflooding Optimization in Irregular Well Patterns Using Streamline Simulation and 3D Visualization. *Processes* **2025**, *13*, 1114. [CrossRef]
26. BuKhamseen, N.Y.; Al-Najem, A.A.; Saffar, A.H. An injection optimization decision-making tool using streamline based fuzzy logic workflow. *J. Pet. Explor. Prod. Technol.* **2022**, *12*, 171–181. [CrossRef]
27. Fakcharoenphol, P.; Charoenwongsa, S.; Kazemi, H.; Wu, Y. The effect of water-induced stress to enhance hydrocarbon recovery in shale reservoirs. *SPE J.* **2013**, *18*, 897–909. [CrossRef]
28. Shi, D.; Cheng, S.; Zhao, D.; Wang, Y.; Liu, X.; Xu, Z. Numerical simulation method for water injection-induced fractures in tight oil reservoirs based on PKN model. *Pet. Geol. Recovery Effic.* **2025**, *32*, 174–185.
29. Liu, F.; Li, Z.; Min, J.; Peng, Y.; Peng, H.; Qin, S.; Liu, Y.; Xiong, J.; Yu, R. Wellbore stability analysis considering rock damage mechanics theory: An integrated experimental and numerical study. *Nat. Gas Ind. B* **2025**, *12*, 674–688. [CrossRef]
30. Deng, X.; Li, J.; Liu, L.; Ren, K. Advances in the Study of Fractured Reservoir Characterization and Modeling. *Geol. J. China Univ.* **2015**, *21*, 306–319. [CrossRef]
31. Van den Hoek, P.J.; Hustedt, B.; Sobera, M.; Mahani, H.; Masfry, R.A.; Snippe, J.; Zwarts, D. Dynamic induced fractures in waterfloods and EOR. In *Proceedings of the SPE Russian Petroleum Technology Conference*; SPE-115204-MS; SPE: Richardson, TX, USA, 2008.
32. Zhu, D.; Griffiths, D.V.; Fenton, G.A.; Huang, J. Probabilistic stability analyses of two-layer undrained slopes. *Comput. Geotech.* **2025**, *182*, 107178. [CrossRef]
33. Lin, H.; Zhang, W.; Guo, S.; Zhang, X.; Wang, L.; Zhang, J. Study on the energy evolution mechanism and fractal characteristics of coal failure under dynamic loading. *ACS Omega* **2025**, *10*, 54710–54719. [CrossRef] [PubMed]
34. Zheng, B.; Zhang, L.; Liu, Y.; Li, Y.; Zhang, Y.; Li, X.; Li, L. Dynamic Response of Fracture Networks and the Evolution of Waterflood Fronts During Fracture-Flooding. *Processes* **2025**, *13*, 3592. [CrossRef]
35. Wang, Y.; Xu, Y.; Li, Y.; Chen, P.; Zou, H.; Li, J.; Sun, Y.; Li, J.; Xu, H.; Wang, J. Numerical Simulation Study on the Mechanism of Pore Volume Expansion and Permeability Enhancement by High-Pressure Water Injection in Low Permeability Reservoirs. *Processes* **2025**, *14*, 48. [CrossRef]

Disclaimer/Publisher's Note: The statements, opinions and data contained in all publications are solely those of the individual author(s) and contributor(s) and not of MDPI and/or the editor(s). MDPI and/or the editor(s) disclaim responsibility for any injury to people or property resulting from any ideas, methods, instructions or products referred to in the content.